



Cite this: RSC Adv., 2019, 9, 25533

Synthesis of novel benzopyran-connected pyrimidine and pyrazole derivatives via a green method using Cu(II)-tyrosinase enzyme catalyst as potential larvicidal, antifeedant activities

Ashraf Abdel-Fattah Mostafa,^{ac} Chidambaram SathishKumar,^b Abdulaziz Abdulrahman Al-Askar,^a Shaban R. M. Sayed,^d Radhakrishnan SurendraKumar^b and Akbar Idhayadhulla^{id}  ^{*b}

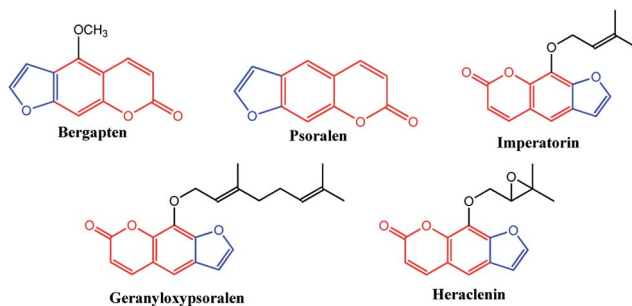
A series of benzopyran-connected pyrimidine (**1a–g**) and benzopyran-connected pyrazole (**2a–i**) derivatives were synthesized via Biginelli reaction using a green chemistry approach. Cu(II)-tyrosinase was used as a catalyst in the synthesis of compounds **1a–g** and **2a–i** via the Biginelli reaction. The as-synthesized compounds were characterized by IR, ¹H NMR, ¹³C NMR, mass spectroscopy, and elemental analysis. The as-synthesized compounds were screened for larvicidal and antifeedant activities. The larvicidal activity was evaluated using the mosquito species *Culex quinquefasciatus*, and the antifeedant activity was evaluated using the fishes of *Oreochromis mossambicus*. The compounds **2a–i** demonstrated lethal effects, killing 50% of second instar mosquito larvae when their LD₅₀ values were 44.17, 34.96, 45.29, 45.28, 75.96, and 28.99 µg mL⁻¹, respectively. Molecular docking studies were used for analysis based on the binding ability of an odorant binding protein (OBP) of *Culex quinquefasciatus* with compound **2h** (binding energy = -6.12 kcal mol⁻¹) and compound **1g** (binding energy = -5.79 kcal mol⁻¹). Therefore, the proposed target compounds were synthesized via a green method using Cu(II)-enzyme as a catalyst to give high yield (94%). In biological screening, benzopyran-connected pyrazole (**2h**) was highly active compared with benzopyran-connected pyrimidine (**1a–g**) series in terms of larvicidal activity.

Received 15th June 2019
 Accepted 18th July 2019

DOI: 10.1039/c9ra04496e
rsc.li/rsc-advances

Benzopyrans (coumarins) are an important group of naturally occurring compounds widely distributed in the plant kingdom and have been produced synthetically for many years for commercial uses.¹ In addition, these core compounds are used as fragrant additives in food and cosmetics.² The commercial applications of coumarins include dispersed fluorescent brightening agents and as dyes for tuning lasers.³ Some important biologically active natural benzopyran (coumarin) derivatives are shown in Fig. 1. Mosquitoes are the vectors for a large number of human pathogens compared to other groups of arthropods.⁴ Their uncontrollable breeding poses a serious threat to the modern humanity. Every year, more than 500 million people are severely affected by malaria. The mosquito

laricide is an insecticide that is specially targeted against the larval life stage of a mosquito. Particularly, the compound bergapten (Fig. 1), which shows the standard of larvicidal activity,⁵ is commercially available, and it was used as a control in this study for larvicidal screening. Moreover, the antifeedant screening defense mechanism makes it a potential candidate for the development of eco-friendly ichthyocides. Coumarin derivatives exhibit a remarkably broad spectrum of biological



^aBotany and Microbiology Dept. College of Science, King Saud University, Riyadh, Kingdom of Saudi Arabia

^bResearch Department of Chemistry, Nehru Memorial College (Affiliated to Bharathidasan University), Puthanampatti-621007, Tiruchirappalli District, Tamil Nadu, South India. E-mail: a.idhayadhulla@gmail.com; idhayadhulla@nmc.ac.in

^cNational Institute of Oceanography and Fisheries, Al-Kanater Fish Research Station, Egypt

^dElectron Microscope Unit, Central Lab., College of Science, King Saud University, Kingdom of Saudi Arabia

Fig. 1 Biologically active natural benzopyran compound.



activities, including antibacterial,^{6,7} antifungal,^{8–10} anticoagulant,¹¹ anti-inflammatory,¹² antitumor,^{13,14} and anti-HIV.¹⁵

Coumarin and its derivatives can be synthesized by various methods, which include the Perkin,¹⁶ Knoevenagel,¹⁷ Wittig,¹⁸ Pechmann,¹⁹ and Reformatsky reactions.

Among these reactions, the Pechmann reaction is the most widely used method for the preparation of substituted coumarins since it proceeds from very simple starting materials and gives good yields of variously substituted coumarins. For example, coumarins can be prepared by using various reagents, such as H_2SO_4 , $POCl_3$,²⁰ $AlCl_3$,²¹ cation exchange resins, trifluoroacetic acid,²² montmorillonite clay,²³ solid acid catalysts,²⁴ W/ZrO_2 solid acid catalyst,²⁵ chloroaluminate ionic liquid,²⁶ and Nafion-H catalyst.²⁷

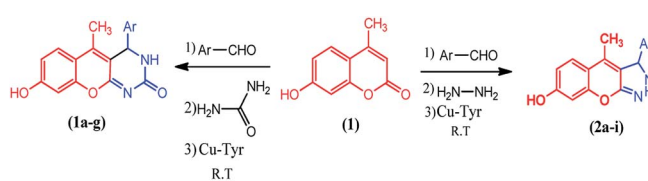
Keeping the above literature observations, coumarin derivatives **1a–g** and **2a–i** are usually prepared with the conventional method involving $CuCl_2 \cdot 2H_2O$ catalysis with using HCl additive. This reduces the yield and also increases the reaction time. To overcome this drawback, we used mushroom tyrosinase as a catalyst without any additive, a reaction condition not reported previously. The as-synthesized compounds were used for the biological screening of larvicidal and antifeedant activities (marine fish). In addition, in this study, we considered the molecular docking studies study based on previous studies for performing the binding ability of hydroxy-2-methyl-4H-pyran-4-one (the root extract of *Senecio laetus* Edgew) with the odorant binding protein (OBP) of *Culex quinquefasciatus*.²⁸

Results and discussion

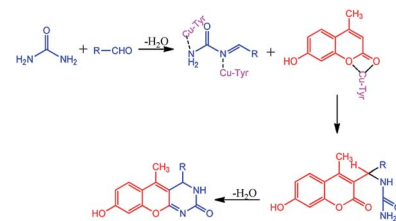
Chemistry

The compounds **1a–g** and **2a–i** were prepared according to the synthesis sequences illustrated in Scheme 1. The proposed mechanism for the formation of the compounds **1a–g** and **2a–i** are shown in Schemes 2 and 3. The Cu-tyrosinase enzyme catalysis performed well to afford yields ranging from 82 to 98% within 2 to 4 min of reaction time compared with other catalysts. The catalyst optimization is shown in Table 1, and the optimization of reaction conditions is shown in Table 2.

All the as-synthesized compounds were characterized by IR, 1H NMR, and ^{13}C NMR analyses. Important assignments of the compounds **1a–g** using the IR spectroscopy include absorption bands at 3174.54–3175.59, 2596.13–2596.89, and 1648.12–1715.02 cm^{-1} , corresponding to the –NH, –C=N and –C=O. The 1H NMR spectrum shows signals at δ 9.19–9.27, 3.97–4.17, and 1.21–1.29 ppm, corresponding to the NH, 4CH protons, and CH_3 . The ^{13}C NMR spectrum shows peaks at δ 160.4, 160.4, and 15.0–15.7 ppm, corresponding to the C=O, C=N, and CH_3 .



Scheme 1 Synthesis of coumarin derivatives **1a–g** and **2a–i**.

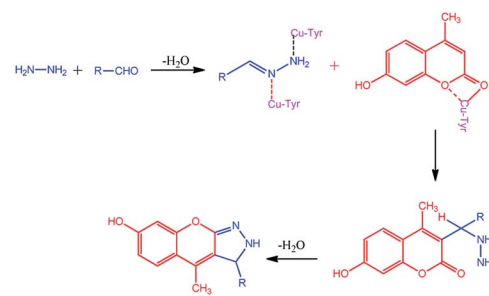


Scheme 2 Proposed mechanism for the formation of **1a–g**.

carbon atoms. The important assignments of the compounds **2a–i** using the IR spectroscopy include absorption bands at 3174.54, 3034, and 2596.13 cm^{-1} , corresponding to the –NH, Ar–H and –C=N. The 1H NMR spectrum shows signals at δ 8.70, 3.99–4.59, and 2.42 ppm, corresponding to the NH, 4CH protons, and CH_3 . The ^{13}C NMR spectrum shows peaks at δ 150.6, 122.3–123.3, and 15.0–15.7 ppm, corresponding to the C=N, C=C, and CH_3 carbon atoms. All compounds were confirmed *via* mass spectroscopy and elemental analysis supported the expected target compounds.

Larvicidal activity

Compounds **1a–g** and **2a–i** were screened for larvicidal activity. Compounds **1a–g** had low activity compared with compounds **2a–i**. The experiments were performed at room temperature. The compound **2h** produced 100% mortality at 100 $\mu g mL^{-1}$. The compound **1g** was the only highly active compound with the LD_{50} value of 46.08 $\mu g mL^{-1}$ in the **1a–g** series. Overall, compounds **1g**, **2a**, **2b**, **2d**, **2e** and **2h** were highly active against *Culex quinquefasciatus* with the LD_{50} values of 46.08, 44.17, 34.96, 45.29, 45.28, and 28.99 $\mu g mL^{-1}$, respectively, than the control bergapten with the LD_{50} value of 73.68 $\mu g mL^{-1}$. Among the as-synthesized compounds **1a–g** and **2a–i**, compound **2h** was highly active against *Culex quinquefasciatus* with the LD_{50} value of 28.99 $\mu g mL^{-1}$ compared with the control bergapten (the LD_{50} value of 73.68 $\mu g mL^{-1}$). The compounds **1g**, **2a**, **2d**, and **2e** were equipotently active (range from 44.17 to 46.08 $\mu g mL^{-1}$) due to the nature of chemical performance; however, some important functional groups displayed the biological activity in different ways. For example, compound **1g** containing pyrimidine with furfuryl gave equipotent activity compared with compound **2a** (electron donating group phenyl with pyrazole), compound **2d** (electron donating group 4-HO-phenyl with



Scheme 3 Proposed mechanism for the formation of **2a–i**.

Table 1 Optimization of the catalyst for compounds (1a)

Entry	Catalyst	Additive	Yield (%)
1	ZnCl ₂	HCl	47
2	SnCl ₂ ·2H ₂ O	HCl	53
3	ZrOCl ₂	HCl	68
4	AlCl ₃	HCl	76
5	CuCl ₂ ·2H ₂ O	HCl	87
6	Cu-tyrosinase enzyme catalysis	Without additive	94

Table 2 Optimization of the reaction conditions for compounds 1a–g and 2a–i

Compd no.	Ar	Catalysis activity, time (min)/yield (%)	
		CuCl ₂	Cu-tyrosinase enzyme catalysis
1a	-Ph	5/87	2/94
1b	-CH=CH-Ph	5/78	3/88
1c	-4-ClC ₆ H ₄	5/83	4/87
1d	-4-OHC ₆ H ₄	5/87	2/89
1e	-3-NO ₂ C ₆ H ₄	5/75	2/85
1f	4-OCH ₃ C ₆ H ₄	5/80	2/89
1g	Furfuryl	5/83	2/89
2a	-Ph	5/72	2/82
2b	-CH=CH-Ph	5/87	2/89
2c	-4-ClC ₆ H ₄	5/89	2/91
2d	-4-OHC ₆ H ₄	5/82	2/92
2e	-3-NO ₂ C ₆ H ₄	5/85	2/95
2f	-N(CH ₃) ₂ C ₆ H ₄	5/89	2/96
2g	4-OCH ₃ C ₆ H ₄	5/71	2/98
2h	Furfuryl	5/83	3/89
2i	Citral	5/79	4/86

pyrazole), and compound 2e (electron withdrawing group 3-NO₂-Ph with pyrazole). The values are summarized in Table 3.

Antifeedant activity (ichthyotoxicity activity)

The as-synthesized compounds 1a–g and 2a–i were screened for the antifeedant activity with many of the compounds showing high toxicity. All the as-synthesized compounds had 100% mortality at 100 µg mL⁻¹ except compounds 1a, 1b, and 2a. Among the as-synthesized compounds 1a–g and 2a–i, the compound 1a was the least toxic with the mortality of 0% at 100 µg mL⁻¹. The compound 1c was highly active with the LD₅₀ value of 18.52 µg mL⁻¹ compared with compounds 1a–g and 2a–i. The compounds 1f, 2c, and 2e (range from 35.07 to 35.98 µg mL⁻¹) had equipotent activity due to the presence of different functional groups, such as electron donating groups at 4-CH₃O-Ph with pyrimidine in compound 1f, electron donating groups at 4-Cl-Ph with pyrazole in compound 2c, and electron withdrawing group 3-NO₂-Ph with pyrazole in compound 2e. The values are summarized in Table 4.

Mosquito larval growth inhibition activities

Considering the regulation of coumarin analogues on growth and metamorphosis, the effect of the compound 2h after a 72 h treatment on the weight gain of larvae and rate of inhibition (Table 5), the duration of the pupal and adult stages and the eclosion rate of the treated *Culex quinquefasciatus* were evaluated at 10 µg mL⁻¹ (Table 6). The weight gain of larvae were controlled by the compound 2h, which gave an inhibitory rate of 55.06%. The effect of the compound 2h on the duration of the pupal and adult stages was evident, and the rate of eclosion was only 40% after treatment with the compound 2h. The results show that the compound 2h exhibited potent inhibitory activity against the growth and development of *Culex quinquefasciatus*.

Table 3 Larvicidal activity of title compounds 1a–g and 2a–i

Compounds	Concentration (µg mL ⁻¹)/mortality ^a (%)				
	10	25	50	100	LD ₅₀ (µg mL ⁻¹)
1a	—	0 ± 0.00	20 ± 0.07	43 ± 0.87	>100
1b	—	0 ± 0.00	14 ± 0.96	33 ± 1.65	>100
1c	—	—	—	—	>100
1d	—	—	0 ± 0.00	20 ± 1.61	>100
1e	—	—	0 ± 0.00	20 ± 0.88	>100
1f	—	—	—	—	>100
1g	18 ± 1.87	40 ± 1.21	60 ± 0.56	80 ± 1.54	46.08
2a	18 ± 1.20	40 ± 1.87	60 ± 0.67	84 ± 0.00	44.17
2b	16 ± 1.87	40 ± 1.61	60 ± 1.67	80 ± 0.09	34.96
2c	—	—	0 ± 0.00	20 ± 1.14	>100
2d	18 ± 0.95	42 ± 1.38	60 ± 1.42	80 ± 1.23	45.29
2e	20 ± 1.76	40 ± 1.23	62 ± 1.94	80 ± 1.11	45.28
2f	0 ± 0.00	20 ± 0.67	44 ± 1.47	60 ± 2.12	75.96
2g	—	0 ± 0.00	8 ± 1.63	20 ± 1.42	>100
2h	46 ± 1.33	62 ± 1.34	84 ± 1.35	100 ± 0.00	28.99
2i	—	0 ± 0.00	10 ± 1.34	20 ± 1.34	>100
Bergapten	11 ± 2.05	25 ± 1.90	41 ± 1.65	63 ± 0.58	73.68

^a Values are the means of three replicates ± SD.



Table 4 Antifeedant activity of title compounds **1a–g** and **2a–i**

Compounds	Concentration ($\mu\text{g mL}^{-1}$)/mortality ^a (%)				
	10	25	50	100	LD_{50} ($\mu\text{g mL}^{-1}$)
1a	—	—	—	—	>100
1b	0 ± 0.00	10 ± 1.23	24 ± 0.96	40 ± 1.65	>100
1c	34 ± 1.23	68 ± 1.54	80 ± 1.42	100 ± 0.00	18.52
1d	14 ± 1.35	38 ± 1.42	60 ± 1.67	100 ± 0.00	32.63
1e	24 ± 1.56	46 ± 1.23	80 ± 1.78	100 ± 0.00	30.28
1f	18 ± 1.12	40 ± 1.32	60 ± 1.42	100 ± 0.00	35.07
1g	20 ± 1.87	38 ± 1.21	62 ± 0.56	100 ± 0.00	36.54
2a	0 ± 0.00	20 ± 1.87	42 ± 0.67	80 ± 1.78	59.97
2b	10 ± 1.87	32 ± 1.61	60 ± 1.67	100 ± 0.00	41.87
2c	20 ± 1.20	42 ± 1.42	68 ± 1.65	100 ± 0.00	35.53
2d	24 ± 0.95	60 ± 1.38	80 ± 1.42	100 ± 0.00	25.58
2e	14 ± 1.76	32 ± 1.23	64 ± 1.94	100 ± 0.00	35.98
2f	28 ± 1.20	46 ± 0.67	68 ± 1.47	100 ± 0.00	33.72
2g	12 ± 1.42	38 ± 1.87	70 ± 1.63	100 ± 0.00	31.56
2h	24 ± 1.33	40 ± 1.34	74 ± 1.35	100 ± 0.00	33.75
2i	20 ± 1.42	42 ± 1.23	60 ± 1.34	100 ± 0.00	34.52

^a Values are the means of three replicates ± SD.

Molecular docking

The docking process involves two basic steps: the prediction of the ligand conformation and assessment of the binding affinity. These two steps are related to sampling methods and scoring schemes respectively. Docking studies were accomplished for compounds **1g** and **2h** in order to calculate their binding affinities against 3OGN protein using the AutoDock4 (version 4.2.6) software. The 3D structure of the ligand **2h** is shown in Fig. 2. The 3D structure of the 3OGN protein is shown in Fig. 3. The results were examined based on the binding energies of the docked complexes. AutoDock4 generated 10 conformers for each ligand. The selection of the best conformer was based on the smallest binding energy between the ligand and the protein. After docking, the ligands were ranked according to their binding energies.

Docked results using the AutoDock4 software

The selected ligand **2h** was docked against 3OGN protein using the AutoDock4 software. The ball and stick representation of the 3OGN-**2h** docked complex is shown in Fig. 4a. The molecular surface representation of the 3OGN-**2h** docked complex is shown in Fig. 4b. The best-selected pose of the 3OGN-**2h** docked complex (binding energy $-6.12 \text{ kcal mol}^{-1}$) with binding site

Table 6 The effect of the title compound **2h** on the growth and development of mosquito larvae

Compound	<i>Culex quinquefasciatus</i> ^a		
	Duration of pupae (h)	Duration of adult (h)	Rate of eclosion (%)
2h ^b	70.1 ± 1.32	25.1 ± 2.34	40 ± 3.10
Control ^c	65.5 ± 1.28	24.2 ± 1.98	90 ± 2.80

^a Values are the means of three replicates ± SD. ^b The concentration of **2h** was $10 \mu\text{g mL}^{-1}$. ^c Control does not contain the compounds.

residues is shown in Fig. 4c. The hydrogen bonds and the types of contacts involved in the 3OGN-**2h** docked complex are shown in Fig. 4d. It was observed that ASP-70 and LYS-106 are involved in hydrogen bond interactions and the residues VAL-71, TYR-97, TYR-97 and PRO-98 are involved in van der Waals interactions. Then, the selected ligand **1g** was docked against the 3OGN. The ball and stick representation of 3OGN-**1g** docked complex is shown in Fig. 5a. The molecular surface representation of the 3OGN-**1g** docked complex is shown in Fig. 5b. The best-selected pose of the 3OGN-**1g** docked complex (binding energy $-5.79 \text{ kcal mol}^{-1}$) with binding site residues is shown in Fig. 5c.

Table 5 The effect of the title compound **2h** on the growth of mosquito larvae

Compound	<i>Culex quinquefasciatus</i> ^a		Weight gain (mg)	Inhibition (%)
	0 h	72 h		
2h ^b	100.28 ± 1.20	102.14 ± 1.33	3.86 ± 1.14	55.06 ± 1.42
Control ^c	100.06 ± 1.21	108.65 ± 0.67	8.59 ± 1.11	—

^a Values are the means of three replicates ± SD. ^b The concentration of **2h** was $10 \mu\text{g mL}^{-1}$. ^c Control does not contain the compounds.



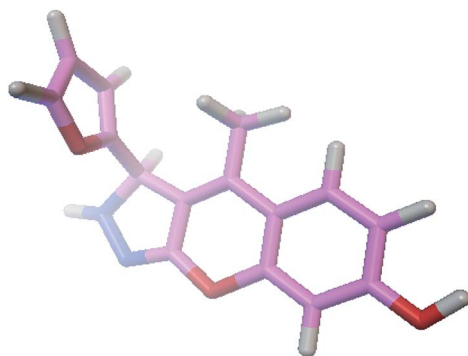


Fig. 2 3D structure of the compound 2h.

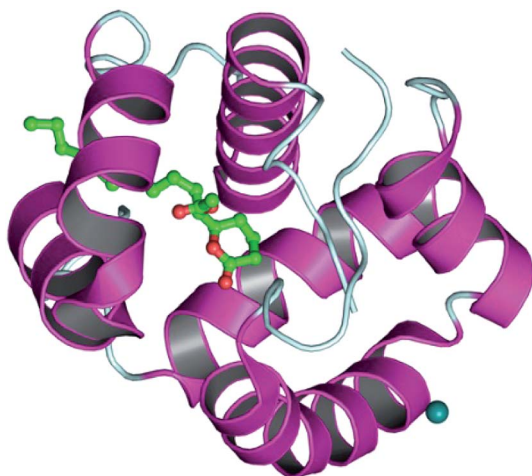


Fig. 3 3D structure of the 3OGN mosquito odorant binding protein.

The hydroxyl bonds and the types of contacts involved in the 3OGN-**1g** docked complex are shown in Fig. 5d. It was observed that ASP-78 and LEU-15 are involved in hydrogen bond interactions and the residues GLU-14, PRO-81 and ASN-82 are involved in van der Waals interactions. The compound **2h** has the highest binding affinity with the mosquito odorant binding protein 3OGN compared with compound **1g**. The molecular docking characterizations for compound **2h** are listed in Table 7, while those for **1g** are listed in Table 8.

Structure-activity relationship

The as-synthesized compounds are compared for the structure and activity relationship, as shown in Fig. 6. The larvicidal activities of the as-synthesized compounds are compared with those of the control bergapten. The larvicidal activity in the presence of pyrazole moiety at the five-membered ring in compound **2h** is highly active with the LD_{50} value of $28.99 \mu\text{g mL}^{-1}$ than the five-membered ring at control bergapten with the LD_{50} value of $73.68 \mu\text{g mL}^{-1}$.

The larvicidal activity in the presence of pyrimidine moiety with the six-membered ring in compound **1g** was highly active with the LD_{50} value of $46.08 \mu\text{g mL}^{-1}$ than the five-membered ring in bergapten with the LD_{50} value of $73.49 \mu\text{g mL}^{-1}$. The

presence of natural aldehyde scaffolds in the title compound shows high larvicidal and antifeedant activities. The presence of the furfuraldehyde scaffold in **2h** shows high larvicidal activity with the LD_{50} value of $28.99 \mu\text{g mL}^{-1}$ than that in the compounds **1a-g** and **2a-i**. The presence of 4-Cl-phenyl scaffold in **1c** shows high antifeedant activity with the LD_{50} value of $18.52 \mu\text{g mL}^{-1}$ than that in the compounds **1a-g** and **2a-i**.

Experimental

General

The chemicals 7-hydroxy-4-methylcoumarin, tyrosinase, and bergapten were purchased from Sigma-Aldrich and used without further purification. Melting points were recorded in open capillary tubes and were uncorrected. The IR spectra (KBr) were recorded in KBr on a Shimadzu 8201 pc (4000–400 cm^{-1}). The ^1H NMR and ^{13}C NMR spectra were recorded on a Bruker DRX-300 MHz. Elemental analysis (C, H, and N) was performed using an Elemental analyzer model (Varian EL III). The purity of the compounds was checked *via* thin layer chromatography (TLC) with silica gel plates.

General method for the preparation of 8-hydroxy-5-methyl-4-phenyl-3,4-dihydro-2H-chromeno[2,3-*d*]pyrimidin-2-one (**1a**)

The mixture of 7-hydroxy-4-methyl-2H-chromen-2-one (0.001 mol, 0.17 g), substituted aldehyde (0.003 mol), urea (0.003 mol, 0.18 g), and Cu(II)-tyrosinase enzyme (0.5 g) were mixed in a mortar. Then, 2 mL of 50 mM potassium phosphate buffer (pH 6.0) was added and filtered. The insoluble product was washed with excess ice-cold water, and then filtered and dried. The product was confirmed *via* TLC. The product was washed in ethanol to get pure product. The same method was followed for the synthesis of compounds **1b-g**.

White solid; mw: 306.32; mp 164 °C; IR (cm^{-1}): 3174.54 (NH), 3074.57 (Ph-CHstr), 3034 (Ar-H), 2596.43 (C=N), 1612.5 (C=O); ^1H NMR (300 MHz, DMSO- d_6): δ 10.5 (1H, s, OH), 8.70 (1H, s, NH), 7.33 (2H, dd, J = 7.33 Hz, J = 7.37 Hz, phenyl), 7.26 (1H, d, J = 6.21 Hz, phenyl), 7.23 (2H, dd, J = 7.31 Hz, J = 7.35 Hz, phenyl), 7.04 (1H, d, J = 6.21 Hz, phenyl), 6.45 (1H, s, phenyl), 6.21 (1H, d, J = 6.21 Hz, phenyl), 5.13 (1H, d, J = 6.21 Hz, -CH), 2.35 (3H, s, -CH₃); ^{13}C NMR (300 MHz, DMSO- d_6): 160.4 (1C, C=O), 160.4 (1C, C=N), 159.1 (1C, -C-OH), 155.7 (1C, -C-O-), 143.3, 128.5, 127.2, 126.9, 126.7, 108.4, 107.9, 99.5 (10C, Ar ring), 136.4 (1C, -C-CH₃), 112.8 (1C, -C=C-CH₃), 42.2 (1C, -C-NH), 15.6 (1C, -CH₃); EI-MS: 307.10 (M^+ , 20%); elemental analysis (C₁₈H₁₄N₂O₃): calculated: C, 70.58; H, 4.61; N, 9.15%; found: C, 70.56; H, 4.62; N, 9.16%.

8-Hydroxy-5-methyl-4-styryl-3,4-dihydro-2H-chromeno[2,3-*d*]pyrimidin-2-one (**1b**)

Light yellow solid; mw: 332.35; mp 146 °C; IR (cm^{-1}): 3174.54 (NH), 3074.57 (Ph-CHstr), 3034 (Ar-H), 2596.43 (C=N), 1612.5 (C=O); ^1H NMR (300 MHz, DMSO- d_6): δ 10.5 (1H, s, OH), 8.70 (1H, s, NH), 7.40 (2H, dd, J = 7.33 Hz, J = 7.37 Hz, phenyl), 7.33 (1H, d, J = 6.21 Hz, phenyl), 7.24 (2H, dd, J = 7.31 Hz, J = 7.35 Hz, phenyl), 7.04 (1H, d, J = 6.21 Hz, phenyl), 6.56 (1H, d, J



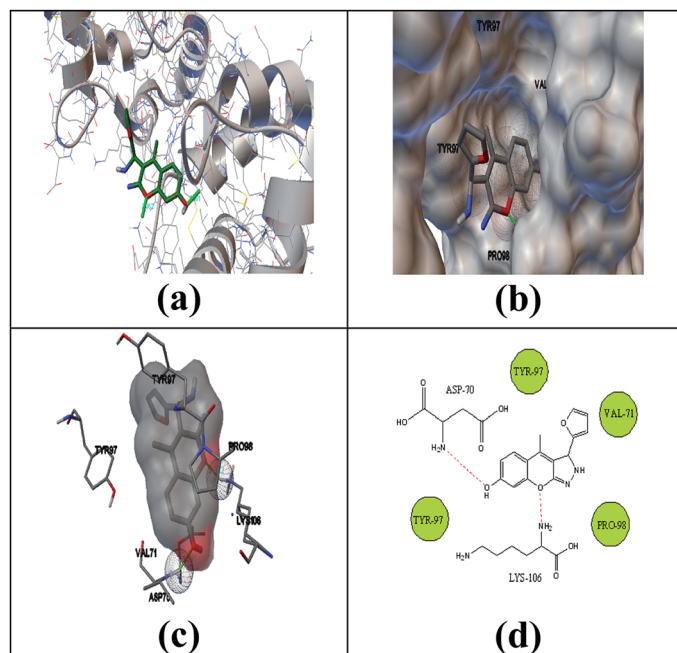


Fig. 4 Ball and stick (a), molecular surface (b), 3D (c), and 2D (d) interaction modes of compound **2h** within the binding site of the mosquito odorant protein 3OGN.

δ = 6.21 Hz, $-\text{CH}$), 6.45 (1H, s, phenyl), 6.21 (1H, d, J = 6.21 Hz, phenyl), 6.19 (1H, d, J = 6.21 Hz, $-\text{CH}$), 4.96 (1H, d, J = 6.21 Hz, $-\text{CH}$), 2.42 (3H, s, $-\text{CH}_3$); ^{13}C NMR (300 MHz, DMSO- d_6): 160.4 (1C, C=O), 160.4 (1C, C=N), 159.1 (1C, $-\text{C}-\text{OH}$), 155.7 (1C, $-\text{C}-\text{O}-$), 136.4 (1C, $-\text{C}-\text{CH}_3$), 136.4, 128.6, 128.5, 127.9, 127.4, 108.4, 107.9, 99.5 (10C, Ar ring), 129.5 (1C, $-\text{C}=\text{C}$), 123.3 (1C, $-\text{C}=\text{C}$), 112.8 (1C, $-\text{C}=\text{C}-\text{CH}_3$), 41.6 (1C, $-\text{C}-\text{NH}$), 15.7 (1C, $-\text{CH}_3$); EI-MS: 333.12 (M^+ , 22%); elemental analysis ($\text{C}_{20}\text{H}_{16}\text{N}_2\text{O}_3$):

calculated: C, 72.28; H, 4.85; N, 8.43%; found: C, 72.27; H, 4.86; N, 8.45%.

4-(4-chlorophenyl)-8-hydroxy-5-methyl-3,4-dihydro-2H-chromeno[2,3-*d*]pyrimidin-2-one (**1c**)

Brown solid; mw: 340.76; mp 178 °C; IR (cm^{-1}): 3174.54 (NH), 3074.57 (Ph-CHstr), 3034 (Ar-H), 2596.43 (C=N), 1612.5 (C=O); ^1H NMR (300 MHz, DMSO- d_6): δ 10.5 (1H, s, OH), 8.70 (1H, s,

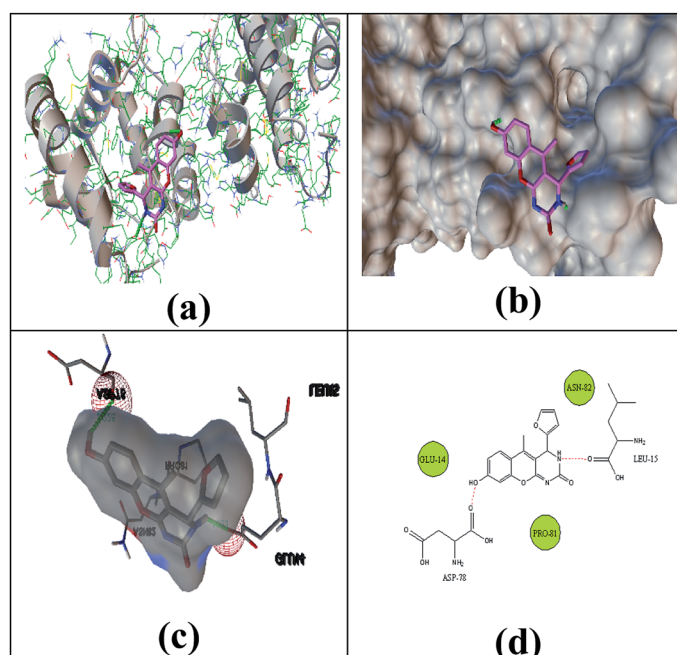


Fig. 5 Ball and stick (a), molecular surface (b), 3D (c), and 2D (d) interaction modes of compound **1g** within the binding site of the mosquito odorant protein 3OGN.



Table 7 Molecular docking for highly active compound 2h

Conformer	Binding energy (kcal mol ⁻¹)	Inhibition constant (K_i) (μM)	Intermolecular energy (kcal mol ⁻¹)	Internal energy (kcal mol ⁻¹)
1	-6.12	32.64	-6.72	-0.48
2	-6.12	32.66	-6.72	-0.48
3	-6.11	33.27	-6.71	-0.47
4	-6.10	33.64	-6.70	-0.48
5	-6.07	35.27	-6.67	-0.47
6	-5.85	51.38	-6.45	-0.48
7	-5.29	132.17	-5.89	-0.47
8	-5.02	208.20	-5.62	-0.47
9	-4.83	287.15	-5.43	-0.38
10	-4.80	303.05	-5.40	-0.47

NH), 7.37 (2H, dd, J = 7.33 Hz, J = 7.37 Hz, phenyl), 7.34 (2H, dd, J = 7.31 Hz, J = 7.35 Hz, phenyl), 7.04 (1H, d, J = 6.21 Hz, phenyl), 6.45 (1H, s, phenyl), 6.21 (1H, d, J = 6.21 Hz, phenyl), 5.13 (1H, d, J = 6.21 Hz, -CH), 2.42 (3H, s, -CH₃); ¹³C NMR (300 MHz, DMSO-d₆): 160.4 (1C, C=O), 160.4 (1C, C=N), 159.1 (1C, -C-OH), 155.7 (1C, -C-O-), 141.4, 132.3, 128.6, 127.2, 126.1, 108.4, 107.9, 99.5 (10C, Ar ring), 136.4 (1C, -C-CH₃), 112.8 (1C, -C=C-CH₃), 42.2 (1C, -C-NH), 15.6 (1C, -CH₃); EI-MS: 342.06 (M⁺, 32%); elemental analysis (C₁₈H₁₃ClN₂O₃): calculated: C, 63.44; H, 3.85; N, 8.22%; found: C, 63.42; H, 3.86; N, 8.23%.

8-Hydroxy-4-(4-hydroxyphenyl)-5-methyl-3,4-dihydro-2H-chromeno[2,3-d]pyrimidin-2-one (1d)

Brown solid; mw: 322.31; mp 172 °C; IR (cm⁻¹): 3174.54 (NH), 3074.57 (Ph-CHstr), 3034 (Ar-H), 2596.43 (C=N), 1612.5 (C=O); ¹H NMR (300 MHz, DMSO-d₆): δ 10.5 (2H, s, OH), 8.70 (1H, s, NH), 7.06 (2H, dd, J = 7.33 Hz, J = 7.37 Hz, phenyl), 7.04 (1H, d, J = 6.21 Hz, phenyl), 6.63 (2H, dd, J = 7.31 Hz, J = 7.35 Hz, phenyl), 6.45 (1H, s, phenyl), 6.21 (1H, d, J = 6.21 Hz, phenyl), 5.13 (1H, d, J = 6.21 Hz, -CH), 2.42 (3H, s, -CH₃); ¹³C NMR (300 MHz, DMSO-d₆): 160.4 (1C, C=O), 160.4 (1C, C=N), 159.1 (1C, -C-OH), 155.7 (1C, -C-O-), 156.5, 135.9, 126.1, 127.2, 115.7, 108.4, 107.9, 99.5 (10C, Ar ring), 136.4 (1C, -C-CH₃), 112.8 (1C, -C=C-CH₃), 42.2 (1C, -C-NH), 15.6 (1C, -CH₃); EI-MS: 323.10 (M⁺, 20%); elemental analysis (C₁₈H₁₄N₂O₄): calculated: C, 67.07; H, 4.38; N, 8.69%; found: C, 67.06; H, 4.40; N, 8.68%.

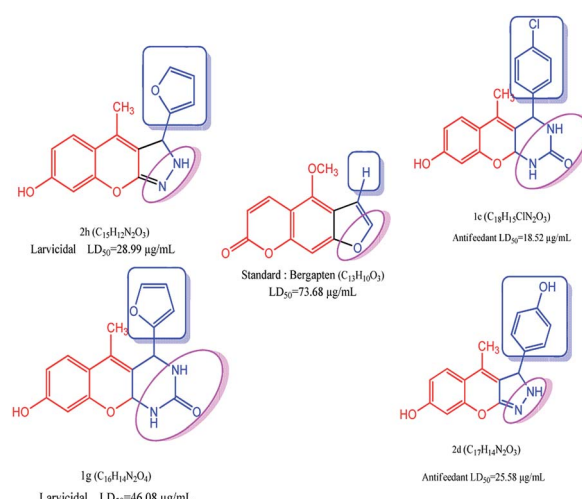


Fig. 6 Structure–activity relationship studies of coumarin derivative.

8-Hydroxy-5-methyl-4-(3-nitrophenyl)-3,4-dihydro-2H-chromeno[2,3-d]pyrimidin-2-one (1e)

White solid; mw: 351.31; mp 108 °C; IR (cm⁻¹): 3174.54 (NH), 3074.57 (Ph-CHstr), 3034 (Ar-H), 2596.43 (C=N), 1612.5 (C=O); ¹H NMR (300 MHz, DMSO-d₆): δ 10.5 (1H, s, OH), 8.70 (1H, s, NH), 8.12 (1H, s, phenyl), 8.07 (1H, d, J = 7.33 Hz, phenyl), 7.62 (1H, d, J = 6.21 Hz, phenyl), 7.59 (1H, dd, J = 7.31 Hz, J = 7.35 Hz, phenyl), 7.04 (1H, d, J = 6.21 Hz, phenyl), 6.45 (1H, s,

Table 8 Molecular docking for low activity compound 1g

Conformer	Binding energy (kcal mol ⁻¹)	Inhibition constant (K_i) (μM)	Intermolecular energy (kcal mol ⁻¹)	Internal energy (kcal mol ⁻¹)
1	-5.79	57.40	-6.38	-0.20
2	-5.76	60.25	-6.36	-0.20
3	-5.73	63.54	-6.32	-0.20
4	-5.71	65.63	-6.30	-0.07
5	-5.69	69.10	-6.28	-0.20
6	-5.66	71.39	-6.25	-0.20
7	-5.61	77.81	-6.20	-0.20
8	-5.34	121.82	-5.94	-0.20
9	-4.99	220.99	-5.58	-0.20
10	-4.86	272.58	-5.46	-0.20



phenyl), 6.21 (1H, d, J = 6.21 Hz, phenyl), 5.13 (1H, d, J = 6.21 Hz, -CH), 2.42 (3H, s, -CH₃); ¹³C NMR (300 MHz, DMSO-d₆): 160.4 (1C, C=O), 160.4 (1C, C=N), 159.1 (1C, -C-OH), 155.7 (1C, -C-O-), 147.7, 144.2, 133.0, 129.4, 121.9, 120.7, 127.2, 108.4, 107.9, 99.5 (10C, Ar ring), 136.4 (1C, -C-CH₃), 112.8 (1C, -C=C-CH₃), 41.2 (1C, -C-NH), 15.6 (1C, -CH₃); EI-MS: 352.09 (M⁺, 20%); elemental analysis (C₁₈H₁₃N₃O₅): calculated: C, 61.54; H, 3.73; N, 11.96%; found: C, 61.56; H, 3.72; N, 11.97%.

8-Hydroxy-4-(4-methoxyphenyl)-5-methyl-3,4-dihydro-2H-chromeno[2,3-d]pyrimidin-2-one (1f)

Brown solid; mw: 336.34; mp 180 °C; IR (cm⁻¹): 3174.54 (NH), 3074.57 (Ph-CHstr), 3034 (Ar-H), 2596.43 (C=N), 1612.5 (C=O); ¹H NMR (300 MHz, DMSO-d₆): δ 10.5 (1H, s, OH), 8.70 (1H, s, NH), 7.12 (2H, dd, J = 7.33 Hz, J = 7.37 Hz, phenyl), 7.04 (1H, d, J = 6.21 Hz, phenyl), 6.87 (2H, dd, J = 7.31 Hz, J = 7.35 Hz, phenyl), 6.45 (1H, s, phenyl), 6.21 (1H, d, J = 6.21 Hz, phenyl), 5.13 (1H, d, J = 6.21 Hz, -CH), 3.83 (3H, s, -OCH₃), 2.42 (3H, s, -CH₃); ¹³C NMR (300 MHz, DMSO-d₆): 160.4 (1C, C=O), 160.4 (1C, C=N), 159.1 (1C, -C-OH), 155.7 (1C, -C-O-), 158.6, 135.6, 125.7, 127.2, 114.1, 108.4, 107.9, 99.5 (10C, Ar ring), 136.4 (1C, -C-CH₃), 112.8 (1C, -C=C-CH₃), 55.8 (1C, -OCH₃), 42.2 (1C, -C-NH), 15.6 (1C, -CH₃); EI-MS: 337.11 (M⁺, 21%); elemental analysis (C₁₉H₁₆N₂O₄): calculated: C, 67.85; H, 4.79; N, 8.33%; found: C, 67.84; H, 4.78; N, 8.35%.

4-(Furan-2-yl)-8-hydroxy-5-methyl-3,4-dihydro-2H-chromeno[2,3-d]pyrimidin-2-one (1g)

Black solid; mw: 296.28; mp 208 °C; IR (cm⁻¹): 3174.54 (NH), 3074.57 (Ph-CHstr), 3034 (Ar-H), 2596.43 (C=N), 1612.5 (C=O); ¹H NMR (300 MHz, DMSO-d₆): δ 10.5 (1H, s, OH), 8.70 (1H, s, NH), 7.65 (1H, d, J = 6.21 Hz, furyl), 7.04 (1H, d, J = 6.21 Hz, phenyl), 6.46 (1H, dd, J = 7.33 Hz, J = 7.37 Hz, furyl), 6.45 (1H, s, phenyl), 6.26 (1H, d, J = 6.21 Hz, furyl), 6.21 (1H, d, J = 6.21 Hz, phenyl), 5.13 (1H, d, J = 6.21 Hz, -CH), 2.42 (3H, s, -CH₃); ¹³C NMR (300 MHz, DMSO-d₆): 160.4 (1C, C=O), 160.4 (1C, C=N), 159.1 (1C, -C-OH), 155.7 (1C, -C-O-), 152.5, 142.1, 127.2, 110.6, 108.4, 107.9, 106.7, 99.5 (8C, Ar ring), 136.4 (1C, -C-CH₃), 112.8 (1C, -C=C-CH₃), 43.4 (1C, -C-NH), 15.0 (1C, -CH₃); EI-MS: 297.08 (M⁺, 18%); elemental analysis (C₁₆H₁₂N₂O₄): calculated: C, 64.86; H, 4.08; N, 9.46%; found: C, 64.87; H, 4.10; N, 9.43%.

General method for preparation of 4-methyl-3-phenyl-2,3-dihydrochromeno[2,3-c]pyrazol-7-ol (2a)

The mixture of 7-hydroxy-4-methyl-2H-chromen-2-one (0.001 mol, 0.17 g), substituted aldehyde (0.003 mol, 0.3 mL), hydrazine hydrate (0.003 mol, 0.1 mL), and Cu(II)-tyrosinase enzyme (0.5 mL) is mixed together in a mortar. Then 2 mL of 50 mM potassium phosphate buffer (pH 6.0) was added and filtered. The insoluble product was washed with excess of ice-cold water filtered and dried. The product was confirmed by TLC. The product was washed in ethanol to get pure product. The same method was followed to the synthesis of other compounds **2b-i**.

Black solid; mw: 278.31; mp 112 °C; IR (cm⁻¹): 3174.54 (NH), 3074.57 (Ph-CHstr), 3034 (Ar-H), 2596.43 (C=N); ¹H NMR (300

MHz, DMSO-d₆): δ 10.5 (1H, s, OH), 8.70 (1H, s, NH), 7.33 (2H, dd, J = 7.33 Hz, J = 7.37 Hz, phenyl), 7.26 (1H, d, J = 6.21 Hz, phenyl), 7.23 (2H, dd, J = 7.31 Hz, J = 7.35 Hz, phenyl), 7.04 (1H, d, J = 6.21 Hz, phenyl), 6.45 (1H, s, phenyl), 6.21 (1H, d, J = 6.21 Hz, phenyl), 4.59 (1H, d, J = 6.21 Hz, -CH), 2.42 (3H, s, -CH₃); ¹³C NMR (300 MHz, DMSO-d₆): 159.1 (1C, -C-OH), 155.7 (1C, -C-O-), 150.6 (1C, C=N), 143.3, 128.5, 127.2, 126.9, 126.7, 108.4, 107.9, 99.5 (10C, Ar ring), 137.2 (1C, -C-CH₃), 122.3 (1C, -C=C-CH₃), 45.8 (1C, -C-NH), 15.6 (1C, -CH₃); EI-MS: 279.11 (M⁺, 19%); elemental analysis (C₁₇H₁₄N₂O₂): calculated: C, 73.37; H, 5.07; N, 10.07%; found: C, 73.36; H, 5.06; N, 10.09%.

4-Methyl-3-styryl-2,3-dihydrochromeno[2,3-c]pyrazol-7-ol (2b)

Red solid; mw: 304.34; mp 194 °C; IR (cm⁻¹): 3174.54 (NH), 3074.57 (Ph-CHstr), 3034 (Ar-H), 2596.43 (C=N); ¹H NMR (300 MHz, DMSO-d₆): δ 10.5 (1H, s, OH), 8.70 (1H, s, NH), 7.40 (2H, dd, J = 7.33 Hz, J = 7.37 Hz, phenyl), 7.33 (1H, d, J = 6.21 Hz, phenyl), 7.24 (2H, dd, J = 7.31 Hz, J = 7.35 Hz, phenyl), 7.04 (1H, d, J = 6.21 Hz, phenyl), 6.56 (1H, d, J = 6.21 Hz, -CH), 6.45 (1H, s, phenyl), 6.21 (1H, d, J = 6.21 Hz, phenyl), 6.19 (1H, d, J = 6.21 Hz, -CH), 3.99 (1H, d, J = 6.21 Hz, -CH), 2.42 (3H, s, -CH₃); ¹³C NMR (300 MHz, DMSO-d₆): 159.1 (1C, -C-OH), 155.7 (1C, -C-O-), 150.6 (1C, C=N), 137.2 (1C, -C-CH₃), 136.4, 128.6, 128.5, 127.9, 127.2, 108.4, 107.9, 99.5 (10C, Ar ring), 129.5 (1C, -C=C), 123.3 (1C, -C=C), 122.3 (1C, -C=C-CH₃), 45.4 (1C, -C-NH), 15.7 (1C, -CH₃); EI-MS: 305.12 (M⁺, 21%); elemental analysis (C₁₉H₁₆N₂O₂): calculated: C, 74.98; H, 5.30; N, 9.20%; found: C, 74.97; H, 5.31; N, 9.18%.

3-(4-chlorophenyl)-4-methyl-2,3-dihydrochromeno[2,3-c]pyrazol-7-ol (2c)

Yellow solid; mw: 312.75; mp 174 °C; IR (cm⁻¹): 3174.54 (NH), 3074.57 (Ph-CHstr), 3034 (Ar-H), 2596.43 (C=N); ¹H NMR (300 MHz, DMSO-d₆): δ 10.5 (1H, s, OH), 8.70 (1H, s, NH), 7.37 (2H, dd, J = 7.33 Hz, J = 7.37 Hz, phenyl), 7.34 (2H, dd, J = 7.31 Hz, J = 7.35 Hz, phenyl), 7.04 (1H, d, J = 6.21 Hz, phenyl), 6.45 (1H, s, phenyl), 6.21 (1H, d, J = 6.21 Hz, phenyl), 4.59 (1H, d, J = 6.21 Hz, -CH), 2.42 (3H, s, -CH₃); ¹³C NMR (300 MHz, DMSO-d₆): 159.1 (1C, -C-OH), 155.7 (1C, -C-O-), 150.6 (1C, C=N), 141.4, 132.3, 128.6, 127.2, 126.1, 108.4, 107.9, 99.5 (10C, Ar ring), 137.2 (1C, -C-CH₃), 122.3 (1C, -C=C-CH₃), 45.8 (1C, -C-NH), 15.6 (1C, -CH₃); EI-MS: 314.06 (M⁺, 32%); elemental analysis (C₁₇H₁₃ClN₂O₂): calculated: C, 65.29; H, 4.19; N, 8.96%; found: C, 65.27; H, 4.20; N, 8.97%.

3-(4-hydroxyphenyl)-4-methyl-2,3-dihydrochromeno[2,3-c]pyrazol-7-ol (2d)

Yellow solid; mw: 294.30; mp 232 °C; IR (cm⁻¹): 3174.54 (NH), 3074.57 (Ph-CHstr), 3034 (Ar-H), 2596.43 (C=N); ¹H NMR (300 MHz, DMSO-d₆): δ 10.5 (2H, s, OH), 8.70 (1H, s, NH), 7.06 (2H, dd, J = 7.33 Hz, J = 7.37 Hz, phenyl), 7.04 (1H, d, J = 6.21 Hz, phenyl), 6.63 (2H, dd, J = 7.31 Hz, J = 7.35 Hz, phenyl), 6.45 (1H, s, phenyl), 6.21 (1H, d, J = 6.21 Hz, phenyl), 4.59 (1H, d, J = 6.21 Hz, -CH), 2.42 (3H, s, -CH₃); ¹³C NMR (300 MHz, DMSO-d₆): 159.1 (1C, -C-OH), 155.7 (1C, -C-O-), 150.6 (1C, C=N), 156.5, 135.9, 126.1, 127.2, 115.7, 108.4, 107.9, 99.5 (10C, Ar



ring), 137.2 (1C, $-C-CH_3$), 122.3 (1C, $-C=C-CH_3$), 45.8 (1C, $-C-NH$), 15.6 (1C, $-CH_3$); EI-MS: 295.10 (M^+ , 19%); elemental analysis ($C_{17}H_{14}N_2O_3$): calculated: C, 69.38; H, 4.79; N, 9.52%; found: C, 69.39; H, 4.81; N, 9.51%.

4-Methyl-3-(3-nitrophenyl)-2,3-dihydrochromeno[2,3-*c*]pyrazol-7-ol (2e)

Yellow solid; mw: 323.30; mp 198 °C; IR (cm^{-1}): 3174.54 (NH), 3074.57 (Ph-CHstr), 3034 (Ar-H), 2596.43 (C=N); 1H NMR (300 MHz, DMSO-d₆): δ 10.5 (1H, s, OH), 8.70 (1H, s, NH), 8.12 (1H, s, phenyl), 8.07 (1H, d, J = 7.33 Hz, phenyl), 7.62 (1H, d, J = 6.21 Hz, phenyl), 7.59 (1H, dd, J = 7.31 Hz, J = 7.35 Hz, phenyl), 7.04 (1H, d, J = 6.21 Hz, phenyl), 6.45 (1H, s, phenyl), 6.21 (1H, d, J = 6.21 Hz, phenyl), 4.59 (1H, d, J = 6.21 Hz, $-CH$), 2.42 (3H, s, $-CH_3$); ^{13}C NMR (300 MHz, DMSO-d₆): 159.1 (1C, $-C-OH$), 155.7 (1C, $-C-O-$), 150.6 (1C, C=N), 147.7, 144.2, 133.0, 129.4, 121.9, 120.7, 127.2, 108.4, 107.9, 99.5 (10C, Ar ring), 137.2 (1C, $-C-CH_3$), 122.3 (1C, $-C=C-CH_3$), 44.8 (1C, $-C-NH$), 15.6 (1C, $-CH_3$); EI-MS: 324.09 (M^+ , 20%); elemental analysis ($C_{17}H_{13}N_3O_4$): calculated: C, 63.16; H, 4.05; N, 13.00%; found: C, 63.15; H, 4.03; N, 13.01%.

3-(4-(dimethylamino)phenyl)-4-methyl-2,3-dihydrochromeno[2,3-*c*]pyrazol-7-ol (2f)

Red solid; mw: 321.37; mp 78 °C; IR (cm^{-1}): 3174.54 (NH), 3074.57 (Ph-CHstr), 3034 (Ar-H), 2596.43 (C=N); 1H NMR (300 MHz, DMSO-d₆): δ 10.5 (1H, s, OH), 8.70 (1H, s, NH), 7.05 (2H, dd, J = 7.33 Hz, J = 7.37 Hz, phenyl), 7.04 (1H, d, J = 6.21 Hz, phenyl), 6.65 (2H, dd, J = 7.31 Hz, J = 7.35 Hz, phenyl), 6.45 (1H, s, phenyl), 6.21 (1H, d, J = 6.21 Hz, phenyl), 4.59 (1H, d, J = 6.21 Hz, $-CH$), 3.06 (6H, s, $-(CH_3)_2$), 2.42 (3H, s, $-CH_3$); ^{13}C NMR (300 MHz, DMSO-d₆): 159.1 (1C, $-C-OH$), 155.7 (1C, $-C-O-$), 150.6 (1C, C=N), 149.1, 132.8, 127.2, 126.1, 112.7, 108.4, 107.9, 99.5 (10C, Ar ring), 137.2 (1C, $-C-CH_3$), 122.3 (1C, $-C=C-CH_3$), 45.8 (1C, $-C-NH$), 41.3 (2C, $-(CH_3)_2$), 15.6 (1C, $-CH_3$); EI-MS: 322.15 (M^+ , 21%); elemental analysis ($C_{19}H_{19}N_3O_2$): calculated: C, 71.01; H, 5.96; N, 13.08%; found: C, 71.23; H, 5.95; N, 13.07%.

3-(4-methoxyphenyl)-4-methyl-2,3-dihydrochromeno[2,3-*c*]pyrazol-7-ol (2g)

Yellow solid; mw: 308.33; mp 144 °C; IR (cm^{-1}): 3174.54 (NH), 3074.57 (Ph-CHstr), 3034 (Ar-H), 2596.43 (C=N); 1H NMR (300 MHz, DMSO-d₆): δ 10.5 (1H, s, OH), 8.70 (1H, s, NH), 7.12 (2H, dd, J = 7.33 Hz, J = 7.37 Hz, phenyl), 7.04 (1H, d, J = 6.21 Hz, phenyl), 6.87 (2H, dd, J = 7.31 Hz, J = 7.35 Hz, phenyl), 6.45 (1H, s, phenyl), 6.21 (1H, d, J = 6.21 Hz, phenyl), 4.59 (1H, d, J = 6.21 Hz, $-CH$), 3.83 (3H, s, $-OCH_3$), 2.42 (3H, s, $-CH_3$); ^{13}C NMR (300 MHz, DMSO-d₆): 159.1 (1C, $-C-OH$), 155.7 (1C, $-C-O-$), 150.6 (1C, C=N), 158.6, 135.6, 125.7, 127.2, 114.1, 108.4, 107.9, 99.5 (10C, Ar ring), 137.2 (1C, $-C-CH_3$), 122.3 (1C, $-C=C-CH_3$), 55.8 (1C, $-OCH_3$), 45.8 (1C, $-C-NH$), 15.6 (1C, $-CH_3$); EI-MS: 309.12 (M^+ , 20%); elemental analysis ($C_{18}H_{16}N_2O_3$): calculated: C, 70.12; H, 5.23; N, 9.09%; found: C, 70.13; H, 5.21; N, 9.08%.

3-(Furan-2-yl)-4-methyl-2,3-dihydrochromeno[2,3-*c*]pyrazol-7-ol (2h)

Brown solid; mw: 268.27; mp 104 °C; IR (cm^{-1}): 3174.54 (NH), 3074.57 (Ph-CHstr), 3034 (Ar-H), 2596.43 (C=N); 1H NMR (300 MHz, DMSO-d₆): δ 10.5 (1H, s, OH), 8.70 (1H, s, NH), 7.65 (1H, d, J = 6.21 Hz, furyl), 7.04 (1H, d, J = 6.21 Hz, phenyl), 6.46 (1H, dd, J = 7.33 Hz, J = 7.37 Hz, furyl), 6.45 (1H, s, phenyl), 6.26 (1H, d, J = 6.21 Hz, furyl), 6.21 (1H, d, J = 6.21 Hz, phenyl), 4.82 (1H, d, J = 6.21 Hz, $-CH$), 2.42 (3H, s, $-CH_3$); ^{13}C NMR (300 MHz, DMSO-d₆): 159.1 (1C, $-C-OH$), 155.7 (1C, $-C-O-$), 150.6 (1C, C=N), 152.5, 142.1, 127.2, 110.6, 108.4, 107.9, 106.7, 99.5 (8C, Ar ring), 137.2 (1C, $-C-CH_3$), 122.3 (1C, $-C=C-CH_3$), 45.5 (1C, $-C-NH$), 15.0 (1C, $-CH_3$); EI-MS: 269.09 (M^+ , 16%); elemental analysis ($C_{15}H_{12}N_2O_3$): calculated: C, 67.16; H, 5.51; N, 10.44%; found: C, 67.17; H, 5.50; N, 10.45%.

3-(2,6-Dimethylhepta-1,5-dien-1-yl)-4-methyl-2,3-dihydrochromeno[2,3-*c*]pyrazol-7-ol (2i)

Brown solid; mw: 324.42; mp 68 °C; IR (cm^{-1}): 3174.54 (NH), 3074.57 (Ph-CHstr), 3034 (Ar-H), 2596.43 (C=N); 1H NMR (300 MHz, DMSO-d₆): δ 10.5 (1H, s, OH), 8.70 (1H, s, NH), 7.04 (1H, d, J = 6.21 Hz, phenyl), 6.45 (1H, s, phenyl), 6.21 (1H, d, J = 6.21 Hz, phenyl), 5.33 (1H, d, J = 6.21 Hz, $-CH=C$), 5.20 (1H, d, J = 6.21 Hz, $-CH=C$), 3.99 (1H, d, J = 6.21 Hz, $-CH$), 2.42 (3H, s, $-CH_3$), 2.00 (4H, d, J = 6.21 Hz, $-(CH_2)_2$), 1.82 (6H, d, J = 6.21 Hz, $-(CH_3)_2$), 1.70 (3H, d, J = 6.21 Hz, $-CH_3$); ^{13}C NMR (300 MHz, DMSO-d₆): 159.1 (1C, $-C-OH$), 155.7 (1C, $-C-O-$), 150.6 (1C, C=N), 137.2 (1C, $-C-CH_3$), 135.5 (1C, $-C=C-$), 132.0 (1C, $-C=C-$), 123.5 (1C, $-C=C-$), 116.7 (1C, $-C=C-$), 127.2, 108.4, 107.9, 99.5 (4C, Ar ring), 122.3 (1C, $-C=C-CH_3$), 39.8 (1C, $-CH_2-$), 39.3 (1C, $-C-NH$), 26.4 (1C, $-CH_2-$), 24.6 (1C, $-CH_3$), 18.6 (1C, $-CH_3$), 16.5 (1C, $-CH_3$), 15.7 (1C, $-CH_3$); EI-MS: 325.19 (M^+ , 20%); elemental analysis ($C_{20}H_{24}N_2O_2$): calculated: C, 74.04; H, 7.46; N, 8.64%; found: C, 74.05; H, 7.47; N, 8.62%.

Larvicidal activity

The larvicidal screenings were performed according to our previously reported methods.²⁹ The LD₅₀ values of several active compounds were evaluated using probit analysis. The results were analyzed using the statistical software SPSS version 16.0. The larval growth inhibition and regulation against *Culex quinquefasciatus* were determined using the water immersion method³⁰.

Antifeedant activity

Fingerlings (1.5–2.0 cm) of marine-acclimated *Oreochromis mossambicus* were used for evaluating ichthyotoxic potential.³¹

Protein preparation for docking

The mosquito odorant binding protein 3OGN was obtained from the protein data bank (PDB).³² For docking, all water molecules were removed from protein, and hydrogen atoms were added to the refined model using AutoDock Tools (ADT), and finally merging the non-polar hydrogens. The as-prepared



protein was saved in PDB, partial charge (Q), and atom type (T) (PDBQT) formats.

Ligand preparation for docking

The ligand was drawn in the Chem 3D pro software and converted into a protein data bank (PDB) file format using the Open Babel software.³³ The ligands were prepared using AutoDock Tools (ADT). Gasteiger charges were assigned to the ligands. The as-prepared ligands were saved in a PDBQT format. Fig. 2 shows the chemical structure of the ligand **2h**.

Molecular docking

AutoDock4 (version 4.2.6) was used for the molecular docking studies. AutoGrid program supplied with AutoDock4 was used for the preparation of grid maps. The grid box size was set at 76, 94, and 76 Å for x, y, and z respectively. The spacing between the grid points was 1.0 Å. The grid center was set at 8.639, 35.906, and 8.905 Å for x, y, and z, respectively. The Lamarckian genetic algorithm (LGA) was chosen from the ADT tool to search for the best conformers. During the docking process, a maximum of 10 conformers was considered for the ligand. The docking processes were performed with the default parameters of AutoDock 4.³⁴ Population size was set to 150, maximum number of evaluations 2 500 000, the maximum number of generations 27 000, the maximum number of a top individual that automatically survived 1, gene mutation rate 0.02 and crossover rate 0.8. AutoDock4 was produced and run under the windows 7 operating system. All figures with structure representations were generated using a python molecule viewer.

Conclusions

From this present study, as-synthesized compounds showed significant activity in the larvicidal and antifeedant screenings. Cu(II)-tyrosinase enzyme was used as a catalyst for Biginelli reaction to give good yield. Compound **2h** showed significant activity against mosquito larvae and low toxic with eco-friendly ichthycides against antifeedant screening when compared with other compounds. Molecular docking studies were well supported for compound **2h** (binding energy $-6.12 \text{ kcal mol}^{-1}$) with good binding ability (OBP) of *Culex quinquefasciatus*. Therefore, these compounds might be a potential source for developing ecologically significant bioactive compounds, including biodegradable pesticides and biopharmaceuticals.

Conflicts of interest

There are no conflicts to declare.

Acknowledgements

The authors extend their appreciation to the Deanship Scientific Research at King Saud University for funding the work through the Research Group Project No RGP-1438-90.

Notes and references

- 1 K. Othmer, *Kirk-Othmer Encyclopedia of Chemical Technology*, John Wiley & Sons, New York, 5th edn, 2007.
- 2 R. O. Kennedy and R. D. Thornes, *Coumarins: Biology, applications and mode of action*, John Wiley & Sons, New York, 1997.
- 3 M. Zabradnik, *The Production and Application of Fluorescent Brightening Agents*, John Wiley and Sons, New York, 1992.
- 4 E. A. El-Hag, A. H. Nadi and A. A. Zaitoon, *Phytother. Res.*, 1999, **13**, 388–392.
- 5 Z. Wang, J. R. Kim, M. Wang, S. Shu and Y. J. Ahu, *Pest Manage. Sci.*, 2012, **68**, 1041–1047.
- 6 A. M. El-Agrody, M. S. Abd El-Latif, N. A. El-Hady, A. H. Fakery and A. H. Bedair, *Molecules*, 2001, **6**, 519–527.
- 7 S. M. De Souza, F. Delle Monache and A. Z. Smânia, *Z. Naturforsch., C: J. Biosci.*, 2005, **60**, 693–700.
- 8 H. C. Marcondes, T. T. De Oliveira, J. G. Taylor, M. Hamoy, A. L. Neto, V. J. De Mello and T. J. J. Nagem, *J. Chem.*, 2015, 241243.
- 9 C. Montagner, S. M. De Souza, C. Groposoa, F. Delle Monache, E. F. Smânia and A. Smânia, *Z. Naturforsch., C: J. Biosci.*, 2008, **63**, 21–28.
- 10 A. F. El-Farargy, *Egypt. J. Pharm. Sci.*, 1991, **32**, 625–628.
- 11 I. Manolov and N. D. Danchev, *Eur. J. Med. Chem.*, 1995, **30**, 531–535.
- 12 A. A. Emmanuel-Giota, K. C. Fylaktakidou, D. J. Hadjipavlou-Litina, K. E. Litinas and D. N. Nicolaides, *Heterocycl. Chem.*, 2001, **38**, 717–722.
- 13 L. Raev, E. Voinov, I. Ivanov and D. Popov, *Pharmazie*, 1990, **45**, 696–702.
- 14 Z. M. Nofal, M. El-Zahar and S. Abd El-Karim, *Molecules*, 2000, **5**, 99–113.
- 15 L. Xie, Y. Tukeuchi, L. M. Consetino and K. Lee, *J. Med. Chem.*, 1999, **42**, 2662–2672.
- 16 B. J. Donnelly, D. M. X. Donnelly and A. M. O. Sullivan, *Tetrahedron*, 1968, **24**, 2617–2622.
- 17 F. Bigi, L. Chesini, R. Maggi and G. Sartori, *J. Org. Chem.*, 1999, **64**, 1033–1035.
- 18 I. Yavari, R. Hekmat-shoar and A. Zonouzi, *Tetrahedron Lett.*, 1998, **39**, 2391–2392.
- 19 E. V. O. Jhon and S. S. Israelstam, *J. Org. Chem.*, 1961, **26**, 240–242.
- 20 S. Z. Ahmed and R. D. Desai, *Proc. Indian Acad. Sci. Sect. A*, 1937, **5**, 277–284.
- 21 A. K. Das Gupta, R. M. Chatterje and K. R. Das, *J. Chem. Soc. C*, 1969, **1**, 29–33.
- 22 L. L. Woods and J. Sapp, *J. Org. Chem.*, 1962, **27**, 3703–3705.
- 23 G. K. Biswas, K. Basu, A. K. Barua and P. Bhattacharya, *Indian J. Chem., Sect. B: Org. Chem. Incl. Med. Chem.*, 1992, **31**, 628–672.
- 24 A. J. Hoefnagel, E. A. Gunnewegh, R. S. Downing and H. V. Bekkum, *J. Chem. Soc., Chem. Commun.*, 1995, **2**, 225–228.
- 25 B. M. Reddy, V. R. Reddy and D. Giridhar, *Synth. Commun.*, 2001, **31**, 3603–3607.



26 A. C. Khandekar and B. M. Khadikar, *Synlett*, 2002, 152–154.

27 D. D. Chaudhari, *Chem. Ind.*, 1983, 569–572.

28 S. I. Ali and V. Venugopalan, *Nat. Prod. Res.*, 2019, DOI: 10.1080/14786419.2019.1634712.

29 I. A. Arif, A. Ahamed, R. S. Kumar, A. Idhayadhulla and A. Manilal, *Saudi J. Biol. Sci.*, 2019, **26**, 673–680.

30 G. P. Song, D. K. Hu, H. Tian, Y. S. Li, Y. S. Cao, H. W. Jin and Z. N. Cui, *Sci. Rep.*, 2016, **6**, 22977.

31 A. A. Ibrahim Anis, R. Surendra Kumar, A. Idhayadhulla and A. Manilal, *Saudi J. Biol. Sci.*, 2019, **26**, 673–680.

32 H. M. Berman, J. Westbrook, Z. Feng, G. Gilliland, H. Weissig, I. N. Shindyalov and P. E. Bourne, *Nucleic Acids Res.*, 2000, **28**, 235–242.

33 G. M. Morris, R. Huey, W. Lindstrom, M. F. Sanner, R. K. Belew, D. S. Goodsell and A. J. Olson, *J. Comput. Chem.*, 2009, **30**, 1639–1662.

34 N. M. O'Boyle, M. Banck, C. A. James, C. Morley, T. Vandermeersch and G. R. Hutchison, *J. Cheminf.*, 2011, **3**, 33–47.

